14th European Workshop on White Dwarfs
ASP Conference Series, Vol. 334, 2005
D. Koester, S. Moehler

Subdwarf B Stars from the ESO Supernova Ia Progenitor Survey – Observation versus Theory

T. Lisker,[1,2] U. Heber,[1] R. Napiwotzki,[1,3] N. Christlieb,[4] Z. Han,[5] D. Homeier,[6] and D. Reimers[4]

[1] *Dr.-Remeis-Sternwarte, Astronomisches Institut der Universität Erlangen-Nürnberg, Sternwartstr. 7, 96049 Bamberg, Germany*
[2] *Institute of Astronomy, ETH Zürich, Department of Physics, HPF D8, ETH Hönggerberg, 8093 Zürich, Switzerland*
[3] *Department of Physics & Astronomy, University of Leicester, University Road, Leicester LE1 7RH, UK*
[4] *Hamburger Sternwarte, Universität Hamburg, Gojenbergsweg 112, 21029 Hamburg, Germany*
[5] *The Yunnan Observatory, Academia Sinica, Kunming, 650011, P.R. China*
[6] *Department of Physics and Astronomy, University of Georgia, Athens, GA 30602-2451, USA*

Abstract. We present the analysis of a high-quality sample of optical spectra for 76 sdB stars from the ESO Supernova Ia Progenitor Survey. Effective temperature, surface gravity, and photospheric helium abundance were derived from line profile fits. We demonstrate that our subsample of 52 single-lined sdB stars is a useful tool to compare observation and theory. The predictions of population synthesis models for close binary evolution are compared to our data. We show that the simulations cover the observed parameter range of sdBs, but fail to reproduce the observed distribution in detail.

1. Introduction and Sample Description

Today, there is no difficulty anymore in characterizing in general terms the nature of subdwarf B (sdB) stars: they are core helium burning stars with a canonical mass of $M \approx 0.5\,\mathrm{M}_\odot$, and a very thin hydrogen envelope ($M_{\mathrm{env}} < 0.01\,\mathrm{M}_\odot$). This places them on the very hot end of the horizontal branch, the so-called extreme horizontal branch (EHB). The difficulty lies in understanding where they come from. Several formation scenarios have been proposed, e.g. mass transfer in close binary systems (e.g. Mengel et al. 1976) or a merger of two helium white dwarfs (Iben 1990). In order to constrain present-day sdB formation models like the simulations of Han et al. (2003), a homogeneous observational sample allowing accurate parameter determinations is required. The ESO Supernova Ia Progenitor Survey (SPY, Napiwotzki et al. 2001) provides such a sample, since the optical VLT/UVES spectra of over 1000 white dwarf candidates contain some 140 previously misclassified hot subdwarfs of various types, among them the 76 sdB stars that constitute our working sample. The SPY sdB spectra overcome the limitations of earlier analyses of sdBs (e.g. Saffer et al. 1994; Maxted

et al. 2001; Edelmann et al. 2003): the high resolution (0.36 Å at Hα or better), homogeneity (same instrumental setup and reduction routine), and wavelength coverage (including all Balmer lines) together form a sample of unprecedented quality.

Effective temperatures ($T_{\rm eff}$), surface gravities ($\log g$), and helium abundances ($y = N_{\rm He}/N_{\rm H}$) were determined by fitting simultaneously each hydrogen and helium line to synthetic LTE and NLTE model spectra using a procedure by Napiwotzki et al. (1999). The 76 sdBs of our sample have effective temperatures in the range $20\,000\,{\rm K} < {\rm T_{eff}} < 38\,000\,{\rm K}$, gravities in the interval $4.8 < \log g < 6.0$, and helium abundances ranging from -4.0 to -0.8. See Lisker et al. (2004) for a more detailed description of data reduction and line profile fitting.

We now introduce another important parameter for our later analysis, namely luminosity in units of the Eddington luminosity, which can be derived solely from $T_{\rm eff}$ and $\log g$:

$$\log L/L_{\rm edd} = 4 \times \log T_{\rm eff}/{\rm K} - \log {\rm g/cm\,s^{-2}} - 15.118$$

Here we assume pure electron scattering in a fully ionized hydrogen atmosphere.

2. Sample Quality and Completeness

Before we can use our sample as a tool to test theoretical predictions, we first have to determine the measurement errors, and potential biases. Since SPY took at least two exposures for most of the stars, we used the distribution of differences in the fit results of individual exposures for determining reliable error estimates. This yielded errors of $\Delta T_{\rm eff} = 370\,{\rm K}$, $\Delta \log g = 0.05\,{\rm dex}$, and $\Delta \log y = 0.04$. The subsequent luminosity error is $\Delta \log L/L_{\rm edd} = 0.04\,{\rm dex}$.

Moreover, we have to consider the possibility of systematic biases. These could, for example, originate from the unknown metallicity of the programme stars. We find that adopting a much lower metallicity ($[m/H] = -2$) in the LTE models than the solar value produces only a significant effect at lower temperatures, where it increases $T_{\rm eff}$ by up to 800 K. However, since analyses of high resolution optical spectra of about two dozen bright sdB stars found near-solar iron abundances (Heber et al. 2000; Heber & Edelmann 2004), it follows that the uncertainties introduced by the unknown metallicity are smaller than the errors of the spectroscopic analyses quoted above for the majority of our objects.

As shown by Heber & Edelmann (2004), the imperfections of both LTE and NLTE model atmospheres is another source of systematic error. These authors find that analysis of spectra with our grid of NLTE models leads to a gravity lower by 0.06 dex than derived from our LTE models, while effective temperatures and helium abundances are not affected. By definition, this would mean a systematic increase of $\log L/L_{\rm edd}$ by 0.06 dex. Although not negligible, this effect is small enough to be irrelevant for our conclusions (see Sect. 3.).

Our results from line profile fitting are presented in Fig. 1, where the $T_{\rm eff}$-$\log g$-plot (left), the $T_{\rm eff}$-$\log y$-plot (middle), as well as the cumulative luminosity function (right) are shown. The latter constitutes a useful visualization of the density distribution of our objects on the EHB band. We now have to investigate whether these results are biased by selection effects.

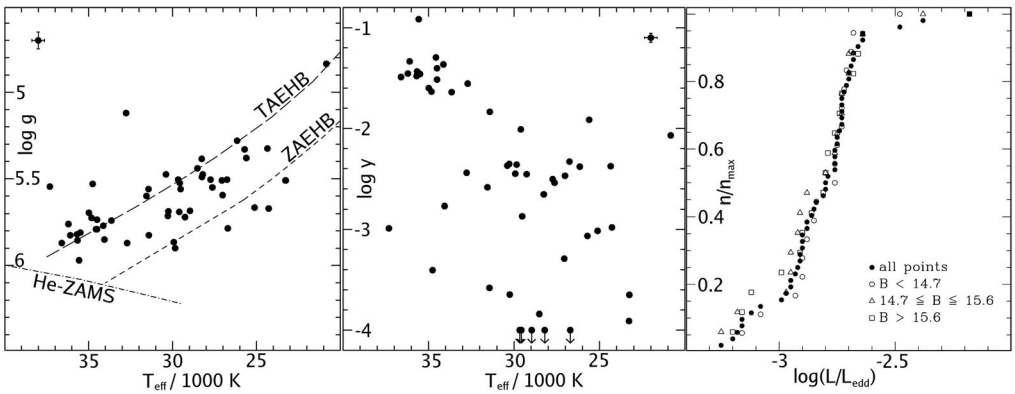

Figure 1. *Left*: Distribution of our sdB sample in the $T_{\rm eff}$-$\log g$-plane. *Middle*: The $T_{\rm eff}$-$\log y$-distribution. *Right*: Cumulative luminosity function for all our objects (filled circles), as well as for three magnitude-selected subsets.

One obvious selection effect always present in observational samples of sdB stars is that sdBs are excluded when they are outshone by a main sequence companion, or when the sdB spectrum is significantly disturbed by the companion light. In the latter case, the mixing of both spectra renders an unbiased analysis impossible. This selection occurs for main sequence companions of spectral type G, K, or earlier, which is why it is known as *GK selection*. After careful exclusion of all sdB+main sequence systems, we are left with 52 single-lined sdB stars. Although the observations cannot be corrected for this effect, theoretical simulations can mimick the same selection, which makes a direct comparison possible.

Another potential bias lies with the flux limitations of the surveys and catalogs (i.e. the Hamburg/ESO Survey, Wisotzki et al. 1996; the Hamburg Quasar Survey, Hagen et al. 1995; McCook & Sion 1999; Napiwotzki 1999) that our programme stars are drawn from. The cumulative luminosity function can be directly used to investigate potential incompleteness effects due to flux limitation. The right panel of Fig. 1 shows the cumulative luminosity functions for three subsets of equal number of stars, selected in increasing magnitude. Any significant incompleteness effects should be revealed by differences in the cumulative functions. However, they obviously agree very well, which clearly demonstrates that our sample does not suffer from such incompleteness, and is therefore a powerful tool for studies of sdB stars. We shall from now on consider the cumulative luminosity function as well as the $T_{\rm eff}$-$\log g$- and the $T_{\rm eff}$-$\log y$-plot as tools to examine the quality of current – and future – models of sdB formation and evolution.

3. Observation versus Theory

The observed sdB distribution is a combined result of the distribution of progenitor systems and the evolution of the sdB stars themselves with time. Hence, one should compare the observations to theoretical models that take both issues into account. Best suited for a comparison are the recent population synthesis

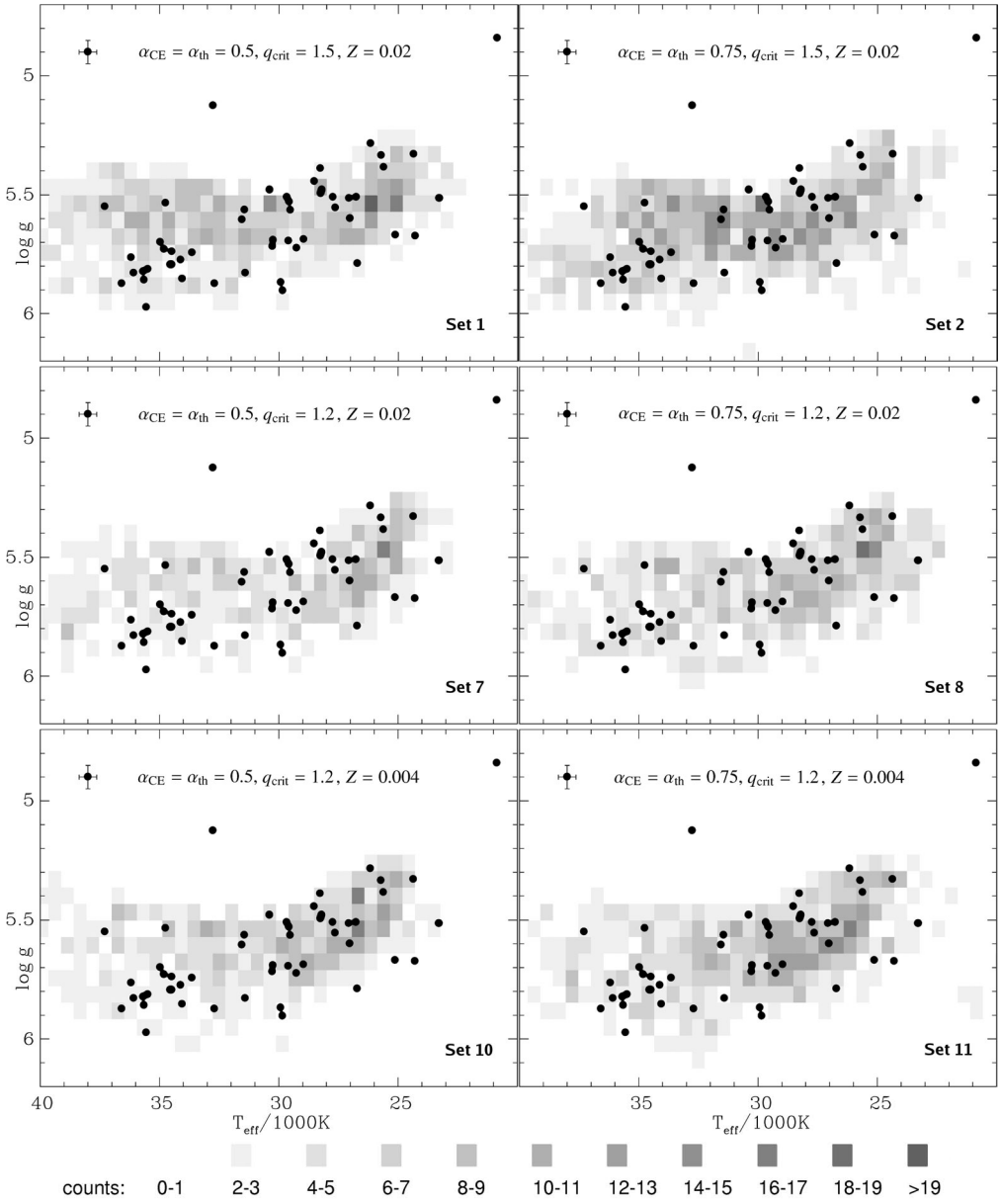

Figure 2. Comparison of the observed $T_{\rm eff}$-log g-distribution with six simulation sets from Han et al. (2003). The latter are shown as shaded $T_{\rm eff}$-log g-boxes, where a higher sdB density per box corresponds to darker shading. The grey scale is shown below the figures. The input parameter values of CE ejection efficiency $\alpha_{\rm CE}$, thermal energy used for ejection $\alpha_{\rm th}$, critical mass ratio for stable mass transfer $q_{\rm crit}$, and metallicity Z are given in each panel.

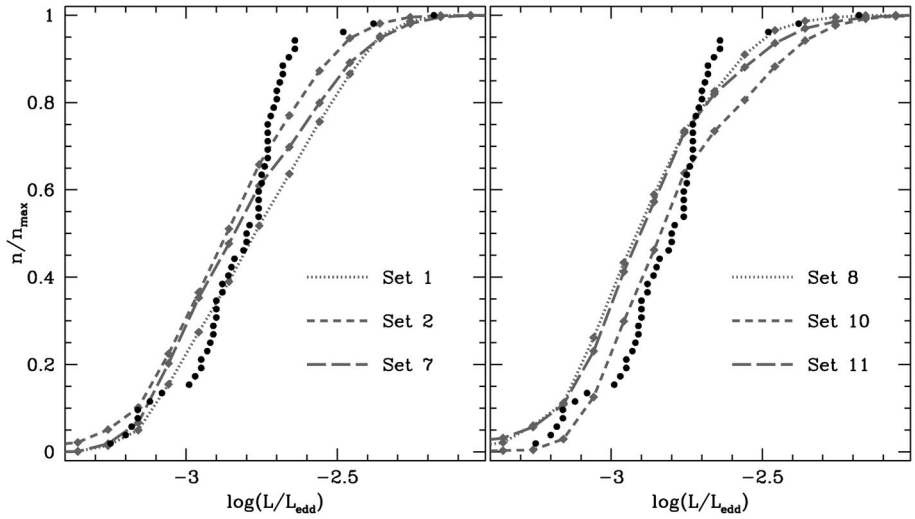

Figure 3. Cumulative luminosity function of our sdB stars as shown in Fig. 1, along with the cumulative functions given by the six HPMM simulation sets from Fig. 2

models for close binary evolution from Han et al. (2003, hereafter HPMM). In these models, core helium burning EHB stars can form via (i) stable Roche lobe overflow, (ii) common envelope (CE) ejection, and (iii) the merging of two helium white dwarfs. By varying input parameters like CE ejection efficiency or initial mass ratio distribution of the progenitor system, HPMM produced twelve different simulation sets of sdB stars. In order to be able to compare these sets to observations, HPMM applied the GK selection criterion discussed above.

We first use the $T_{\rm eff}$-log g-diagram for a visual comparison (see Fig. 2). Lisker et al. (2004) already showed that the models with a CE ejection efficiency of 100% and the ones with an uncorrelated mass ratio of the progenitor binary system fail to match the observed distribution. The remaining six simulation sets all reproduce the observational data resonably well at first glance. However, a closer inspection of Fig. 2 makes clear that the distribution of objects with $T_{\rm eff} > 32\,000$ K differs to some extent from the simulations: (i) these objects have higher gravities than predicted, (ii) a gap between these and the cooler stars can be seen, which is not present in the simulations, and (iii) the simulations extend to hotter temperatures than the observations. The latter point could probably be solved by creating a combined sample of sdB and sdO stars, which is discussed in these proceedings by Ströer et al.

Let us now inspect the cumulative luminosity functions of the various simulation sets (Fig. 3). Although observations and simulations match at the low luminosity end, the HPMM models generally predict a shallower slope than we observe. They are clearly displaced from the observed distribution in the region of higher luminosity, which confirms the differences in the $T_{\rm eff}$-log g-distribution described above.

4. Conclusions

We have demonstrated that our results from the spectroscopic analysis of the SPY sdB sample serve as a high-quality tool to compare observations with present-day and future models of sdB formation. We showed that the Han et al. (2003) binary population synthesis calculations populate the desired parameter range, but do not manage to reproduce the observed distributions satisfyingly. This is probably due to a general lack of knowledge of input physics details. Furthermore, allowing for a single star formation channel in addition to the binary formation scenarios might be worth to consider.

The sample of hot subdwarfs from the SPY survey will allow us to address two important issues. (i) Whether or not all types of hot subdwarfs form through the same channels can be investigated by incorporating the subluminous O stars from SPY into our analysis (see Ströer et al., these proceedings). (ii) The characteristics of all close binaries in the sample will be determined by measuring their periods and mass functions. Napiwotzki et al. (2004) found a binary fraction of about 40% for the SPY subdwarf sample. The analysis of these radial velocity variables is under way (see Karl et al., these proceedings). The resulting distribution of periods and (minimum) masses of the unseen companions will set stringent constraints on the evolutionary models. In addition photometric monitoring will allow to single out main sequence companions in short period systems by searching for their reflection effect (see Maxted et al. 2004). This will constrain the relative weight of different formation channels.

References

Edelmann, H., Heber, U., Hagen, H.-J., et al. 2003, A&A, 400, 939
Hagen, H.-J., Groote, D., Engels, D., & Reimers, D. 1995, A&AS, 111, 195
Han, Z., Podsiadlowski, P., Maxted, P. F. L., & Marsh, T. R. 2003, MNRAS, 341, 669
Heber, U.,& Edelmann, H. 2004, Ap&SS, 291, 341
Heber, U., Reid, I. N., & Werner, K. 2000, A&A, 363, 198
Iben, I. J. 1990, ApJ, 353, 215
Lisker, T., Heber, U., Napiwotzki, R., et al. 2004, A&A, in press (astro-ph/0409136)
Maxted, P. F. L., Morales-Rueda, L., & Marsh, T. R. 2004, Ap&SS, 291, 307
Maxted, P. F. L., Heber, U., Marsh, T. R., & North, R. C. 2001, MNRAS, 326, 1391
McCook, G. P.,& Sion, E. M. 1999, ApJS, 121, 1
Mengel, J. G., Norris, J., & Gross, P. G. 1976, ApJ, 204, 488
Napiwotzki, R. 1999, A&A, 350, 101
Napiwotzki, R., Karl, C. A., Lisker, T.,et al. 2004, Ap&SS, 291, 321
Napiwotzki, R., Christlieb, N., Drechsel, H., et al. 2001, Astronomische Nachrichten, 322, 411
Napiwotzki, R., Green, P. J., & Saffer, R. A. 1999, ApJ, 517, 399
Saffer, R. A., Bergeron, P., Koester, D., & Liebert, J. 1994, ApJ, 432, 351
Werner, K.,& Dreizler, S. 1999, Journal of Computational and Applied Mathematics, 109, 65
Wisotzki, L., Koehler, T., Groote, D., & Reimers, D. 1996, A&AS, 115, 227